processes

MDPI

*Article*

# Biodegradation Kinetic Studies of Phenol and *p*-Cresol in a Batch and Continuous Stirred-Tank Bioreactor with *Pseudomonas putida* ATCC 17484 Cells

**Yen-Hui Lin * and Yi-Jie Gu**

Department of Safety, Health and Environmental Engineering, Central Taiwan University of Science and Technology, 666, Bu-zih Road, Bei-tun District, Taichung 406053, Taiwan; twbob871006@gmail.com
* Correspondence: yhlin1@ctust.edu.tw; Tel.: +886-4-22391647 (ext. 6861)

**Abstract:** The biodegradation of phenol, *p*-cresol, and phenol plus *p*-cresol mixtures was evaluated using *Pseudomonas putida* ATCC 17484 in aerobic batch reactors. Shake-flask experiments were performed separately using growth medium with initial nominal concentrations of phenol (50–600 mg $L^{-1}$) and *p*-cresol (50–600 mg $L^{-1}$) as well as phenol (50–600 mg $L^{-1}$) plus *p*-cresol (50–600 mg $L^{-1}$). The complete degradation of phenol and *p*-cresol was achieved within 48 h and 48–56 h, respectively, for all initial concentrations of phenol and *p*-cresol. The maximum cell growth rate using phenol ($\mu_{max,P}$ = 0.45 $h^{-1}$) was much faster than that using *p*-cresol ($\mu_{max,C}$ = 0.185$^{-1}$ h). The larger $K_i$ value for phenol (310.5 mg $L^{-1}$) revealed that the *P. putida* cells had a higher resistance to phenol inhibition compared with *p*-cresol (243.56 mg $L^{-1}$). A mixture of phenol and *p*-cresol in batch experiments resulted in the complete removal of phenol within 52–56 h for initial phenol concentrations of 50–500 mg $L^{-1}$. The time needed to remove *p*-cresol completely was 48–56 h for initial *p*-cresol concentrations of 50–500 mg $L^{-1}$. In the continuous-flow immobilized cells reactor, the degradation efficiency for phenol and *p*-cresol was 97.6 and 89.1%, respectively, at a stable condition.

**Keywords:** biodegradation; phenol; *p*-cresol; batch reactor; immobilized cells; continuous stirred-tank bioreactor



**Citation:** Lin, Y.-H.; Gu, Y.-J. Biodegradation Kinetic Studies of Phenol and *p*-Cresol in a Batch and Continuous Stirred-Tank Bioreactor with *Pseudomonas putida* ATCC 17484 Cells. *Processes* **2021**, *9*, 133. https://doi.org/10.3390/pr9010133

Received: 16 December 2020
Accepted: 6 January 2021
Published: 9 January 2021



## 1. Introduction

Phenol and its derivatives are toxic organic components often found in various petroleum and chemical industries [1]. Phenol has been regarded as a toxic pollutant to aquatic living organisms imparted as low as concentrations of 0.005 mg $L^{-1}$ [2]. There has been serious environmental concern due to the persistent toxicity of phenol and its derivatives [3]. Much industrial wastewater contains the major phenol and its derivatives such as phenol and cresols [4,5]. Thus, the removal of these phenolic contaminants to a satisfactorily low level in wastewater becomes an urgent task.

Conventional treatments to phenol and its derivatives including physical and chemical methods have major disadvantages such as the cost of operation, production of harmful metabolites, incomplete mineralization of the substances, and high cost involved in disposal of chemical waste sludge. In such cases, biological treatment processes seem promising for the complete mineralization of phenol and its derivatives to carbon dioxide and water with innocuous residues [6]. However, the growth of microorganisms suffers from the inhibition of phenol and its derivatives at higher concentration levels. In order to overcome the inhibition of phenol and its derivatives, the cell acclimation [7], the application of genetically engineered microorganisms [8], and cell immobilization [9,10] have been recommended. Increasing phenol concentrations successively to cultivate phenol-degrading bacteria usually requires long lag times. Masque et al. [7] demonstrated that the degradation of phenol with 1000 mg $L^{-1}$ needed to take 20 days. The use of genetically engineered microorganisms gives the potential for an unanticipated ecological influence

and causes controversy in the application of bioremediation. Thus, cell immobilization gains a better alternative to protect cells from the toxicity of phenol and its derivatives.

Biological treatment processes such as activated sludge system, biofilm process, biological contact oxidation, biofilter process, etc. are always environmentally friendly, highly effective, and economic [11]. In those biological systems, *Pseudomonas putida* as a rod-shaped Gram-negative bacterium has been proved to be effective in removing phenol and its derivatives [12]. A pure culture of *P. putida* ATCC 17484 with high removal efficiency for phenol and *p*-cresol biodegradation in a batch system has been demonstrated [13,14]. González et al. [13] used stirred tank and fluidized-bed bioreactors to degrade phenol through immobilized cells of *P. putida* ATCC 17484. Their experimental results revealed that both bioreactors achieved phenol biodegradation efficiencies higher than 90% even a phenol loading rate in the influent as high as 4 g $L^{-1}$ $d^{-1}$. Loh and Ranganath [15] carried out an external-loop fluidized bed airlift bioreactor (EFBAB) by using *P. putida* ATCC 49451 for the cometabolic biotransformation of 4-chlorophenol (4-CP) in the presence of phenol. Their study found that phenol and 4-CP with feed concentrations of 1600 and 200 mg $L^{-1}$ had been successfully degraded in EFBAB process. The bacterial strain isolated from the contaminated sites by coke-oven effluent was identified as *P. putida* that showed a high capacity in degrading phenol concentration up to 1800 mg $L^{-1}$ and tolerating cyanide up to 340 mg $L^{-1}$ [16].

The biodegradation of toxic substances using entrapped cells has been utilized since 1975 [9]. The immobilized cells have their potential advantages over free cells for the enhancement of biodegradation efficiency in terms of cell reuse and recovery [17]. The biopolymeric gel beads used to entrap microbial cells are well-established approaches for cell immobilization [18]. Banerjee et al. [1] successfully presented phenol biodegradation kinetics by immobilized cells in a batch system. However, the kinetic model system based on the simultaneous biodegradation kinetics of phenol and *p*-cresol in a continuous stirred-tank bioreactor with immobilized cells has never been reported.

The knowledge of dual-substrates biodegradation kinetics by immobilized cells is helpful for the design of process facilities for the simultaneous removal of multiple substrates in wastewater. In this study, *P. putida* ATCC 17484 was entrapped in Ca-alginate gel beads using immobilization methods to evaluate the phenol and *p*-cresol biodegradation kinetics simultaneously. Moreover, the immobilized kinetic model system to describe the simultaneous biodegradation kinetics of phenol and *p*-cresol was developed. The goal of this work was to develop the kinetic model system to describe the biodegradation kinetics of phenol and *p*-cresol simultaneously. The main purposes of this study were to (1) evaluate phenol and *p*-cresol degradation by free *P. putida* cells, respectively; (2) estimate the growth yield and maximum specific growth rate of *P. putida* cells in batch experiments; (3) determine interaction parameters by a sum kinetic equation fitted by experimental data; (4) develop the kinetic model in the immobilized cells system in the continuous stirred bioreactor; (5) conduct continuous-flow experiments to investigate the synchronous biodegradation of phenol and *p*-cresol by alginate-immobilized *P. putida* cells; and (6) compare the experimental data and model prediction for the synchronous biodegradation of phenol and *p*-cresol by alginate-immobilized cells in a continuous stirred-tank bioreactor.

## 2. Kinetic Model Development

### 2.1. Growth Kinetics of Free Cells Batch System

The specific growth rate of cells $\mu$ ($h^{-1}$) obtained from the exponential phase in the batch experiment is expressed as [19,20]

$$\mu = \frac{\ln(X_t / X_0)}{t - t_0} \quad (1)$$

where $X_t$ and $X_0$ are the cell concentration at time $t$ and $t_0$. The value of $\mu$ was determined from the slope of a linear plot of $\ln(X_t/X_0)$ versus time ($t$) in the log-growth phase of the curve.

*P. putida* cells used phenol or *p*-cresol as a sole carbon source, respectively, in a batch culture system. Phenol or *p*-cresol as a substrate displayed an inhibition to cell growth at much higher initial concentrations of phenol or *p*-cresol. Haldane kinetics used to model the cell growth using phenol or *p*-cresol as a substrate, respectively, was represented by the following equation:

$$\mu = \frac{\mu_{\max} \cdot S}{K_s + S + S^2/K_i} \tag{2}$$

where $\mu$ is the specific growth rate ($h^{-1}$), $\mu_{\max}$ is the maximum specific growth rate ($h^{-1}$), $K_s$ is the half-saturated constant of substrate (mg $L^{-1}$), and $K_i$ is the inhibition constant (mg $L^{-1}$).

The experimental data on the substrate degradation at various combinations of initial concentrations of phenol and *p*-cresol were utilized for determining the growth yield of *P. putida* cells according to the following equations [21]:

$$Y = \frac{X - X_0}{S_0 - S} \tag{3}$$

where $Y$ is the growth yield of cells, $X$ and $X_0$ are the cell concentration and initial cell concentration (mg $L^{-1}$), respectively, and $S$ and $S_0$ are the substrate concentration and initial substrate concentration (mg $L^{-1}$), respectively.

Yoon et al. [22] proposed the sum kinetic model to evaluate the interaction parameters ($I_{C,P}$ and $I_{P,C}$) based on the individual specific growth rate.

$$\mu = \frac{\mu_{\max,P} S_P}{K_{s,P} + S_P + S_P^2/K_{i,P} + I_{C,P} S_C} + \frac{\mu_{\max,C} S_C}{K_{s,C} + S_C + S_C^2/K_{i,C} + I_{P,C} S_P} \tag{4}$$

where $P$ and $C$ indicate phenol and *p*-cresol, respectively. $I_{C,P}$ indicates the degree to which *p*-cresol affects the biodegradation of phenol and vice versa. The higher parameter value makes a stronger inhibition on the cells growth [22]. The other bio-kinetic parameters $\mu_{\max}$, $K_s$, and $K_i$ are the same as those obtained from Equation (2) in a single substrate batch system.

### 2.2. Conceptual Basis of Immobilized Cells in the Continuous Stirred-Tank Bioreactor

Figure 1 presents the phenol and *p*-cresol concentration profiles in the bulk liquid, liquid film, and gel bead in the completely-mixed and continuous-flow bioreactors. In the bulk liquid, the phenol and *p*-cresol concentration profiles are flat lines due to a completely-mixed condition occurred in this phase. Then, the phenol and *p*-cresol pass through the liquid film and diffuse into the gel bead to constitute the curved profiles of concentration in the gel bead.

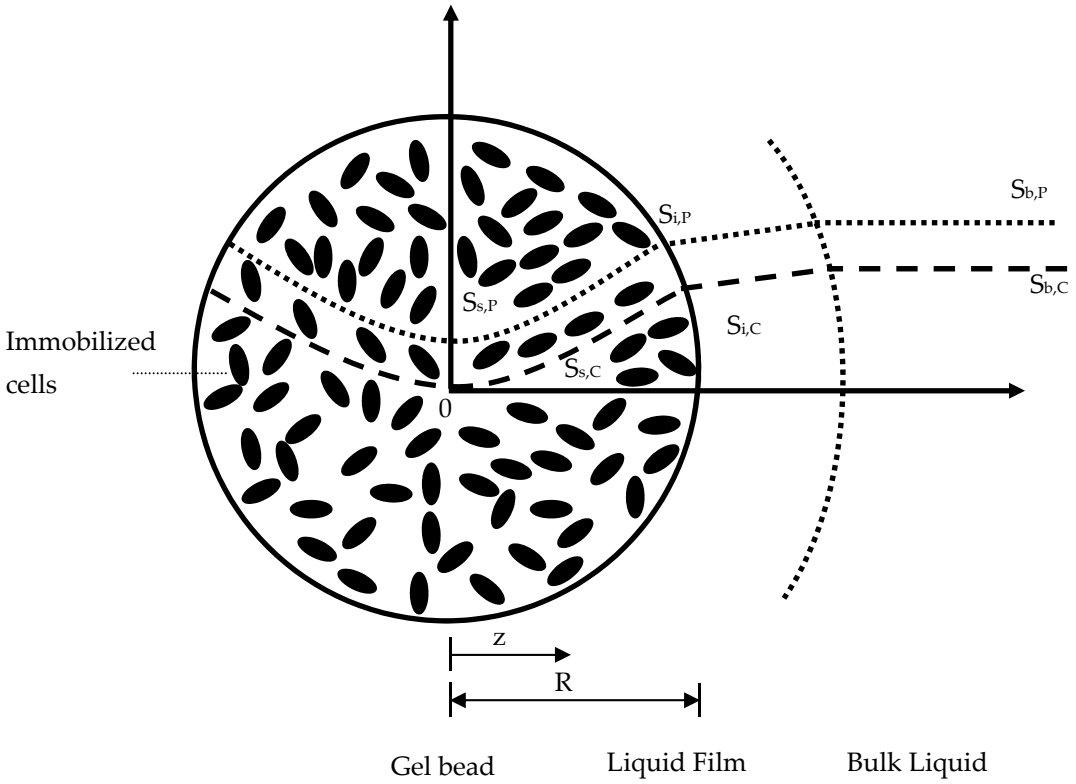


**Figure 1.** Conceptual basis of concentration profiles in an immobilized cells system.

### *2.3. Kinetic Model of the Entrapped Cell in the Continuous Stirred-Tank Bioreactor*

The phenol and *p*-cresol in the bulk liquid diffused into gel beads through the liquid film and were biodegraded by immobilized cells. Diffusion and biodegradation are two fundamental mechanisms occurred simultaneously in this phenomena. According to Fick's law and Haldane's kinetics, the utilization rates of phenol and *p*-cresol in the gel bead with an unsteady-state condition were given as [1,23]:

$$\frac{\partial S_{s,P}}{\partial t} = D_{eP}\left(\frac{\partial^2 S_{s,P}}{\partial z^2} + \frac{2}{z}\frac{\partial S_{s,P}}{\partial z}\right) - \frac{\mu_{\max,P} S_P X_s}{Y_P\left(K_{s,P} + S_P + S_P^2/K_{i,P} + I_{C,P} S_C\right)} \quad (5)$$

$$\frac{\partial S_{s,C}}{\partial t} = D_{eC}\left(\frac{\partial^2 S_{s,C}}{\partial z^2} + \frac{2}{z}\frac{\partial S_{s,C}}{\partial z}\right) - \frac{\mu_{\max,C} S_C X_s}{Y_C\left(K_{s,C} + S_C + S_C^2/K_{i,C} + I_{P,C} S_P\right)} \quad (6)$$

where $S_{s,P}$ and $S_{s,C}$ are the phenol and *p*-cresol concentrations within the gel bead (mg $L^{-1}$), $D_{eP}$ and $D_{eC}$ are the effective diffusivity of phenol and *p*-cresol, respectively, within the porous matrix (cm$^2$ $d^{-1}$), $\mu_{\max,P}$ and $\mu_{\max C}$ are the maximum specific growth rate of cells on phenol and *p*-cresol ($h^{-1}$), respectively, $Y_P$ and $Y_C$ are the growth yield of cells on phenol and *p*-cresol (mg $mg^{-1}$), respectively, $K_{s,P}$ and $K_{s,C}$ are half-saturated constants of phenol and *p*-cresol (mg $L^{-1}$), respectively, $K_{i,P}$ and $K_{i,C}$ are inhibition constants of phenol and *p*-cresol (mg $L^{-1}$), respectively, $I_{C,P}$ and $I_{P,C}$ represent the effect of *p*-cresol on phenol biodegradation and the effect of phenol on *p*-cresol biodegradation, respectively, and $z$ is the radial distance within the bead. The fluxes of phenol and *p*-cresol diffused into the film/bead interface are equivalent to the fluxes diffused out the film/bead interface. The boundary conditions for phenol and *p*-cresol concentration profiles at the bead center and film/bead interface were described as the following equations:

$$\text{BC1}: \ \frac{\partial S_{s,P}}{\partial z} = 0, \ z = 0 \quad (7)$$

$$\text{BC1}: \frac{\partial S_{s,C}}{\partial z} = 0,\ z = 0 \tag{8}$$

$$\text{BC2}: D_{eP}\frac{\partial S_{s,P}}{\partial z} = k_{fP}(S_{b,P} - S_{i,P}),\ z = R \tag{9}$$

$$\text{BC2}: D_{eC}\frac{\partial S_{s,P}}{\partial z} = k_{fC}(S_{b,C} - S_{i,C}),\ z = R. \tag{10}$$

The initial conditions for phenol and *p*-cresol utilization rates in Equations (6) and (7) were expressed by

$$\text{IC1}: S_{s,P} = 0,\ 0 \le z \le R,\ t = 0 \tag{11}$$

$$\text{IC2}: S_{s,C} = 0,\ 0 \le z \le R,\ t = 0. \tag{12}$$

The growth of *P. putida* cells in the bead was written by the following equation:

$$\frac{\partial X_s}{\partial t} = \mu X_s. \tag{13}$$

The initial condition for the growth of cells in the bead can be represented by

$$\text{IC}: X_s = X_0,\ t = 0 \tag{14}$$

where $X_0$ is the initial condition of cells in the bead.

The mass balance of phenol and *p*-cresol in the bulk liquid phase and initial conditions for phenol and *p*-cresol were given by:

$$\frac{dS_{b,P}}{dt} = \frac{Q}{V\varepsilon}(S_{b0,P} - S_{b,P}) - k_{fP}(S_{b,P} - S_{s,P})\frac{3X_w}{V\varepsilon\rho_b R},\ z = R \tag{15}$$

$$\frac{dS_{b,C}}{dt} = \frac{Q}{V\varepsilon}(S_{b0.C} - S_{b,C}) - k_{fC}(S_{b,C} - S_{s,C})\frac{3X_w}{V\varepsilon\rho_b R},\ z = R \tag{16}$$

$$\text{IC1}: S_{b,P} = S_{b0,P} \tag{17}$$

$$\text{IC2}: S_{b,C} = S_{b0,C}. \tag{18}$$

In the above equations, $S_{b,P}$ and $S_{b,C}$ are the concentration of phenol and *p*-cresol in the bulk liquid (mg $L^{-1}$), respectively, $S_{b0,P}$ and $S_{b0,C}$ are the concentrations of phenol and *p*-cresol in the feed (mg $L^{-1}$), $k_{fP}$ and $k_{fC}$ are the external mass transfer coefficients of phenol and *p*-cresol (mg $L^{-1}$), $S_{s,P}$ and $S_{s,C}$ are the concentrations of phenol and *p*-cresol at the liquid/bead interface (mg $L^{-1}$), $Q$ is the influent flow rate ($cm^3$ $d^{-1}$), $V$ is the working volume of the reactor ($cm^3$), $\varepsilon$ is the porosity of the reactor, $X_w$ is the weight of beads (g), $\rho_b$ is the density of the gel beads ($g/cm^3$), and $R$ is the radius of gel beads (cm).

## 3. Materials and Methods

### *3.1. Chemicals*

Phenol and *p*-cresol (>99% purity) purchased from Merck, KGaA, Darmstadt, Germany were of analytical grade in this study. One g of phenol and *p*-cresol, respectively, were dissolved in 1.0 L distilled/deionized water (DIDW) to form the stock solutions. The desired concentration containing phenol or *p*-cresol or phenol plus *p*-cresol was prepared by using stock solutions. All stock solutions are stored at 4 °C prior to use.

### *3.2. Cell Cultivation for Immobilization*

Pure culture of *P. putida* ATCC 17484 with high removal efficiency for phenol and *p*-cresol biodegradation has been demonstrated [14,24,25]. *P. putida* ATCC 17484 grown in mineral salt medium (MSM) [2,26] with 20 mg $L^{-1}$ of phenol as the carbon source was incubated and collected at the stationary phase. Then, the cells were centrifuged at 3000 rpm for 10 min. The phosphate buffer saline with pH 7.4 was used for washing cells. Then, the washed cells were used as inoculum for biodegradation. The flasks contained

100 mL MSM with varying initial concentrations of phenol, *p*-cresol, and phenol plus *p*-cresol, respectively, from 50 to 600 mg $L^{-1}$ were prepared to conduct the batch experiments. The MSM was auto-claved at 121 °C for 15 min, and phenol as well as *p*-cresol were sterilized by a membrane filter.

### 3.3. Entrapment of Cells in Ca-Alginate

Ten mL of centrifuged *P. putida* cells were mixed with 50 mL of sodium alginate of 2% (*w*/*v*) to form the cell–alginate mixture [1]. Then, the cell–alginate mixture was dropped into $CaCl_2$ of 1% (*w*/*v*) to form gel beads with a diameter of 3 mm. The phosphate buffer saline (PBS) was used to wash gel beads three times. Then, the gel beads were immersed in 3 g/L $CaCl_2$ and stored at 4 °C for overnight to strengthen the gel formation [11].

### 3.4. Batch Experiments

The varying initial concentration (50–600 mg $L^{-1}$) of phenol, *p*-cresol, and phenol plus *p*-cresol with 200 mL MSM was conducted in batch mode, respectively. The bio-kinetic parameters were estimated from those batch tests. The flasks were placed in the rotary incubator at 30 °C and 150 rpm to observe the biodegradation of phenol, *p*-cresol, and phenol plus *p*-cresol. Samples were taken from the flasks with a different time interval to measure the concentrations of cells, phenol, and *p*-cresol.

### 3.5. Analysis of P. putida Cells, Phenol and p-Cresol

The optical density (OD) at 600 nm wavelength was used to represent the cell concentration using a UV/vis spectrophotometer. Based on the calibration curve, the linear relationship between cells concentration (X) and $OD_{600}$ was X (mg cell $L^{-1}$) = 343.75 × $OD_{600}$. High-Performance Liquid Chromatograph (HPLC) (Alliance 2695, Waters Corp., Milford, MA, USA) equipped with a UV/vis detector (Waters 2487, Waters Corp., Milford, MA, USA) with an auto-sampler (Waters 2707, Waters Corp., Milford, MA, USA) was setup to analyze the samples. A C18 column with a 150 × 3.9 mm size and packed with 5 µm particle size was applied to analyze the residual phenol and *p*-cresol concentrations. The wavelength was set at 254 nm in the UV/vis detector. The mobile phase containing potassium phosphate and acetonitrile with a volume ratio of 70/30 was used to elute the samples.

### 3.6. Continuous-Flow Bioreactor

A schematic laboratory-scale completely mixed and continuous-flow bioreactor is illustrated in Figure 2. The cylinder shape was composed of glass with an acrylic stand. The shape of the system is cylinder made of glass with an acrylic stand. The bioreactor body was 46.6 cm height and 10 cm diameter. The working volume was 1.568 L as the liquid level was 30 cm. A hydraulic residence time (HRT) was 6 h when the influent flow rate was controlled at 6.272 L $d^{-1}$ in this study. The volume of gel beads was about 0.96 L, which is approximately 40% of the effective volume. The dissolved oxygen was transported by an air compressor with 1 L/min air flow rate. The circulating water bath was employed to control the bioreactor temperature at 30 ± 0.1 °C using the water jacket. The inlet port at the bottom of bioreactor was connected with a digital peristaltic pump using a silicone tubing to provide a flow rate of 11.32 mL $min^{-1}$. The influent feed contained phenol plus *p*-cresol as binary substrates with MSM. The pH value was controlled at 7.0 ± 0.1 by adding PBS in the influent feed.

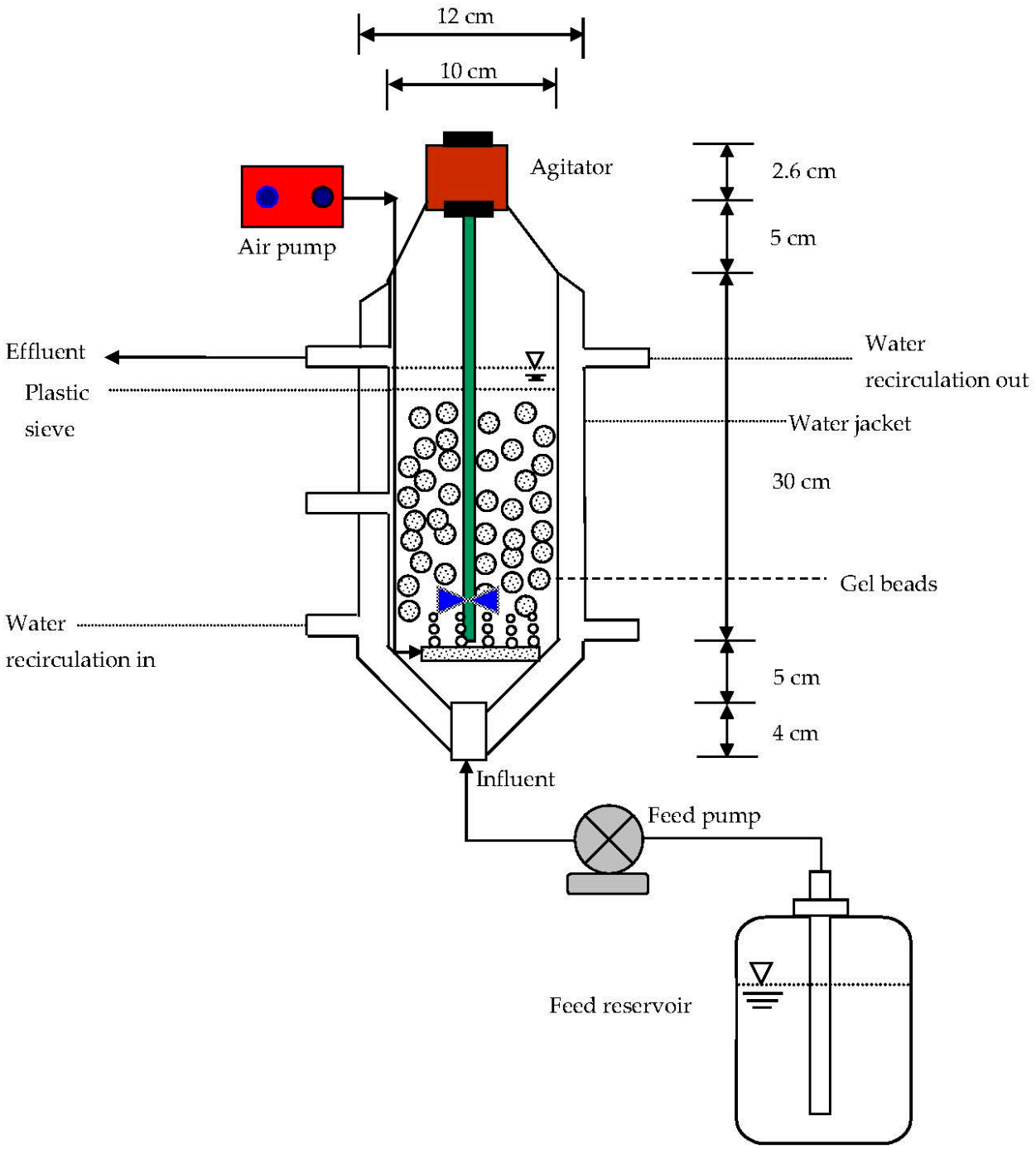


**Figure 2.** A completely mixed and continuous-flow bioreactor.

## 4. Results and Discussion

### *4.1. Biodegradation of Phenol or p-Cresol in Batch Experiments*

Figure 3 plots the phenol biodegradation and cell growth with various initial phenol (50–600 mg $L^{-1}$) and cells concentration (7.68–8.73 mg cell $L^{-1}$). The required time for phenol complete degradation at all levels was about 24 h (Figure 3a). There was no significant lag phase that occurred from 50 to 600 mg L of initial phenol concentration. After 24 h, the cell growth reached a constant value ranging from 24.7 to 211 mg cell $L^{-1}$ under different initial phenol concentration (Figure 3b). The time required for complete phenol degradation by *P. putida* CCRC 14365 was in the range of 6–47 h as the initial phenol concentration increased from 0.27 to 4.25 mM [27]. Kumar et al. [28] conducted a batch

reactor to evaluate the phenol degradation by *P. putida* MTCC 1194. They reported that the cells had the ability to degrade an initial phenol concentration of 1000 mg $L^{-1}$ completely in 162 h. Figure 4a illustrates the *p*-cresol degradation varying from 50 to 600 mg $L^{-1}$. It can be seen that the needed time for the complete biodegradation of *p*-cresol ranged from 24 to 52 h under varying initial *p*-cresol concentrations of 50–600 mg $L^{-1}$. As illustrated in Figure 4b, the lag phase of cells growth was obvious, and the lag time was about 8 h. The time required to achieve a steady-state cell growth ranged from 24 to 52 h. The range of final cell concentration was 21.3 to 176 mg cell $L^{-1}$.

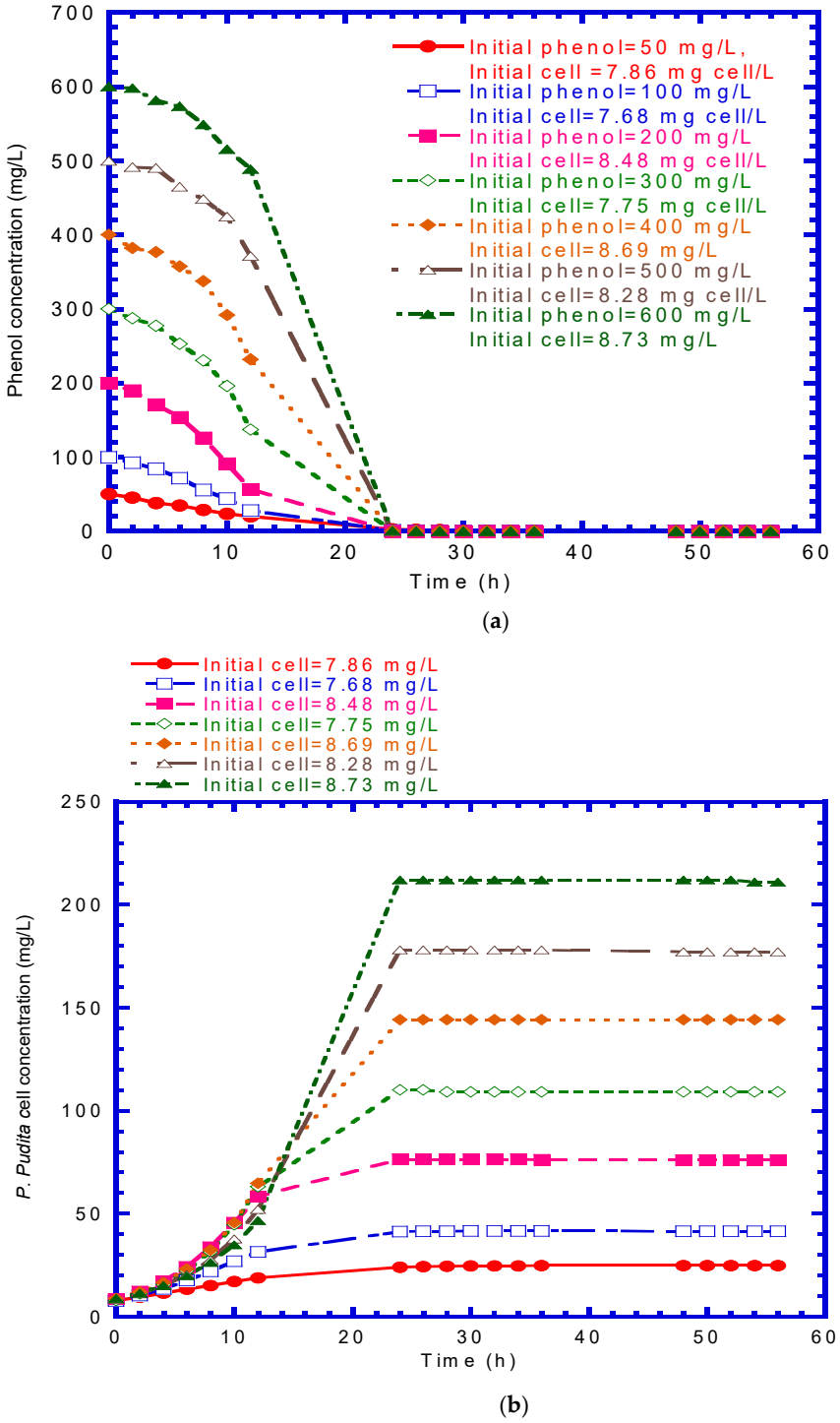


**Figure 3.** Time course of the change in concentration for various concentrations of initial phenol and *P. putida* cells: (**a**) phenol and (**b**) *P. putida* cells.

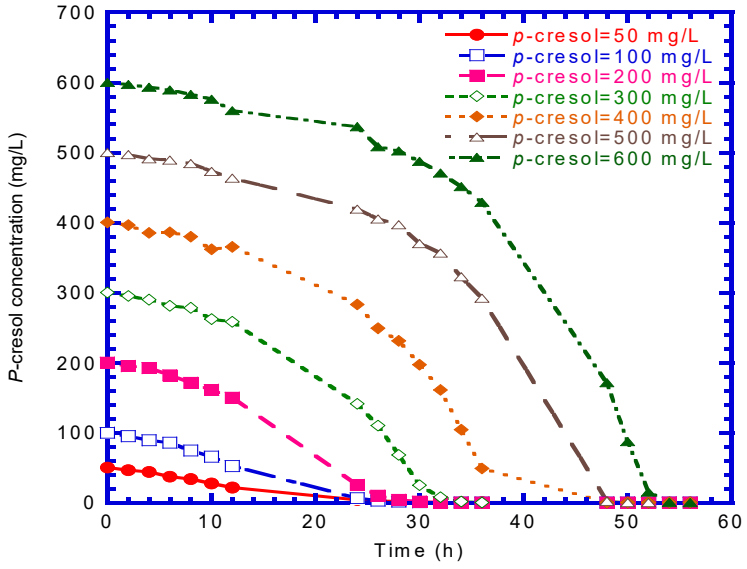


(**a**)

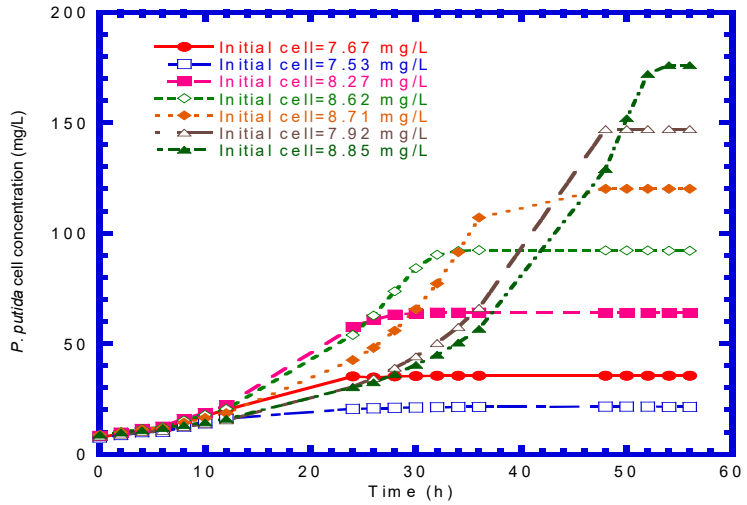


(**b**)

**Figure 4.** Time course of the change in concentration for various concentrations of initial *p*-cresol and *P. putida* cells: (**a**) *p*-cresol and (**b**) *P. putida* cells.

### *4.2. P. putida Cells Growth on Phenol or p-Cresol*

Figure 5a plots $\ln(X/X_0)$ versus time to determine the specific growth rate of the cell on phenol. The specific growth rate on phenol was ranged from 0.0769 to 0.175 $h^{-1}$. Figure 5b illustrates the $\ln(X/X_0)$ plotted with time at varying initial *p*-cresol concentration and cell concentrations. The range of the specific growth rate on *p*-cresol was 0.0515–0.082 $h^{-1}$. As shown in Figures 6 and 7, it is noted that the *P. putida* cells had the maximum specific growth rate as the initial phenol and *p*-cresol concentrations were approximately 220 and 140 mg $L^{-1}$, respectively. The cells growth was inhibited when the initial phenol and *p*-cresol concentrations were greater than 220 and 140 mg $L^{-1}$, respectively. The batch experimental data were fitted by Haldane's kinetics to obtain the bio-kinetic values of $\mu_{max}$ $K_s$ and $K_i$ on phenol and *p*-cresol, respectively, by a non-linear least squares regression method using the Excel software [27]. Haldane's equations for phenol and *p*-cresol with the best-fit bio-kinetic parameters were yielded as follows:

$$\textbf{Phenol: } \mu_P = \frac{0.45 S_P}{221.4 + S_P + S_P^2/310.5} \quad (19)$$

$$\textbf{\textit{P}-cresol: } \mu_C = \frac{0.185 S_C}{65.1 + S_C + S_C^2/243.56} \quad (20)$$

where $\mu_P$ and $\mu_C$ are the specific growth rates of *P. putida* cells on phenol and *p*-cresol, respectively. The $\mu_{max}$, $K_s$, and $K_i$ values for phenol were 0.45 $h^{-1}$, 221.4, and 310.5 mg $L^{-1}$, respectively. The $\mu_{max}$, $K_s$, and $K_i$ values for *p*-cresol were 0.185 $h^{-1}$, 65.1, and 243.56 mg $L^{-1}$, respectively. The cells with a higher maximum specific growth rate utilized phenol more faster than *p*-cresol. In addition, the larger $K_s$ value on phenol resulted in a lower affinity of cells to phenol. The higher $K_i$ value on phenol (310.5 mg $L^{-1}$) displayed that the cells had a stronger resistance to phenol inhibition than to *p*-cresol (243.56 mg $L^{-1}$). A higher inhibition to cells growth by *p*-cresol than that by phenol was observed, as the initial concentration was over 200 mg $L^{-1}$. The phenol biodegradation by *P. putida* shows the $\mu_{max}$ value for phenol (0.45 $h^{-1}$) falling between 0.33 and 0.90 $h^{-1}$ according to the literature survey [29–31]. The $K_i$ value for phenol obtained here (310.5 mg $L^{-1}$) also falls within the ranges of 54.1–669.0 mg $L^{-1}$ [29–31]. The $K_s$ value (221.4 mg $L^{-1}$) for phenol obtained in this study was close to that obtained from the study of Banerjee et al. [32]. The $K_s$ value obtained in their study was 190.8 mg $L^{-1}$.

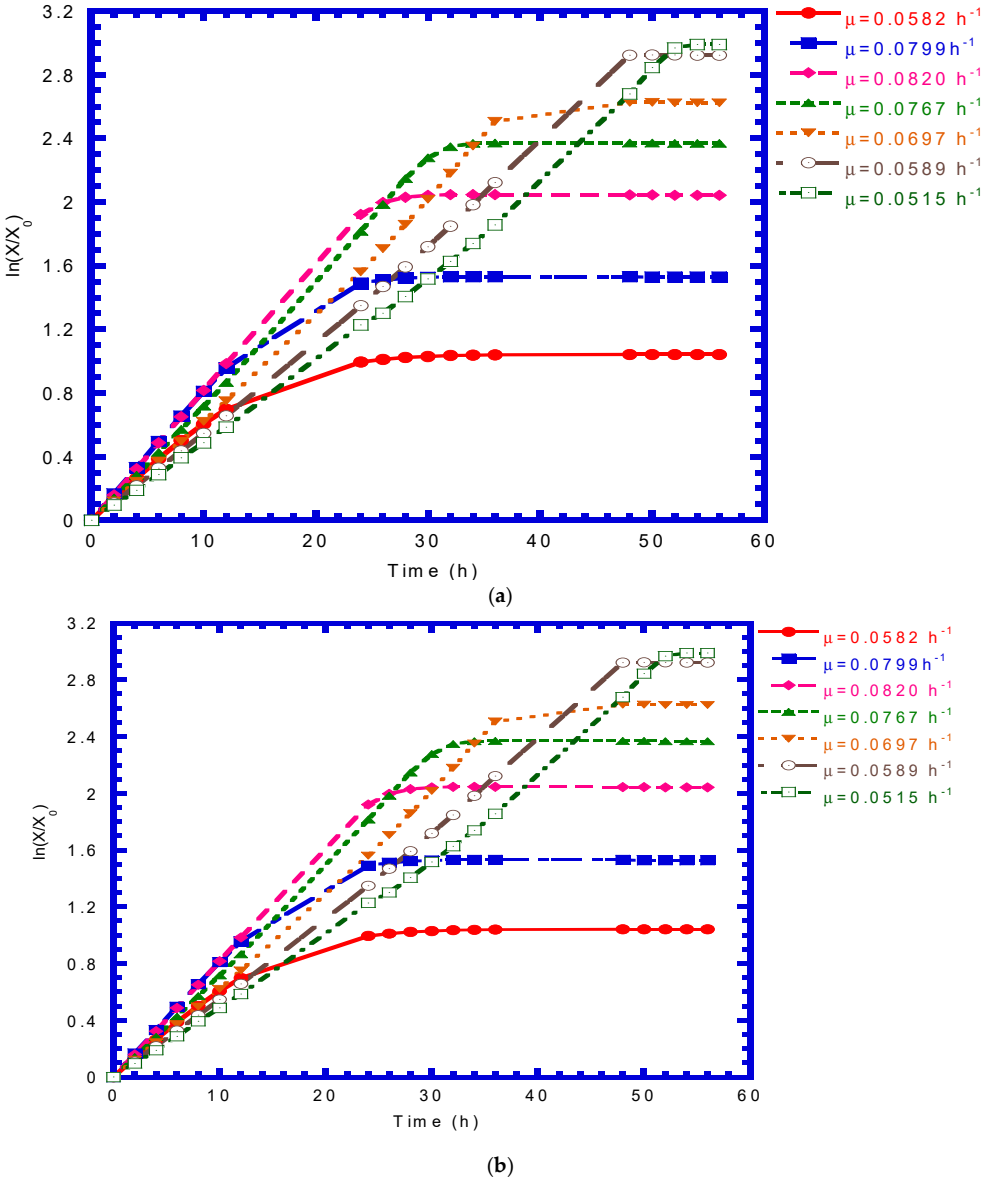


**Figure 5.** Batch experiments to evaluate the specific growth rate under different initial single-substrate and cells concentrations: (**a**) phenol (**b**) *p*-cresol.

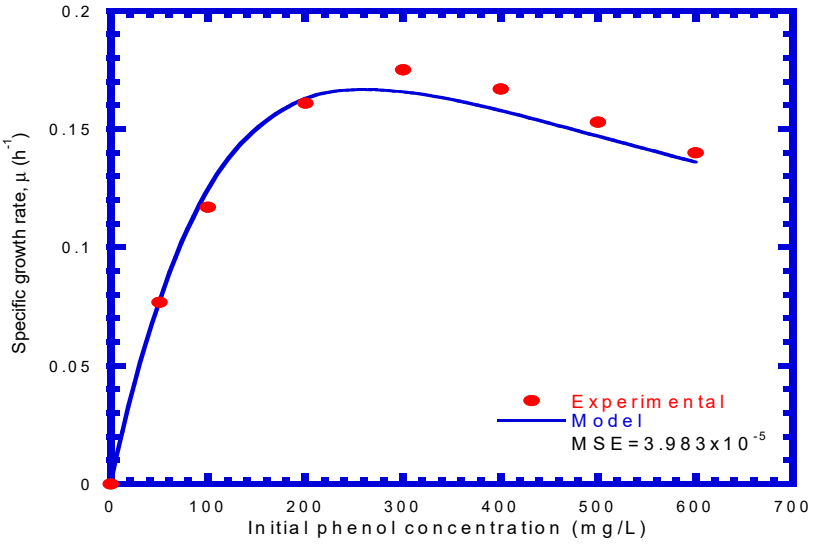


**Figure 6.** Specific growth rate of cells varied with various initial phenol concentrations. Haldane kinetics was fitted to the experimental data using the least-squares methodology. The maximum specific growth rate ($\mu_{max}$) is 0.45 $h^{-1}$, the phenol half-saturation constant is 221.4 mg/L, and the phenol inhibition constant is 310.5 mg/L.

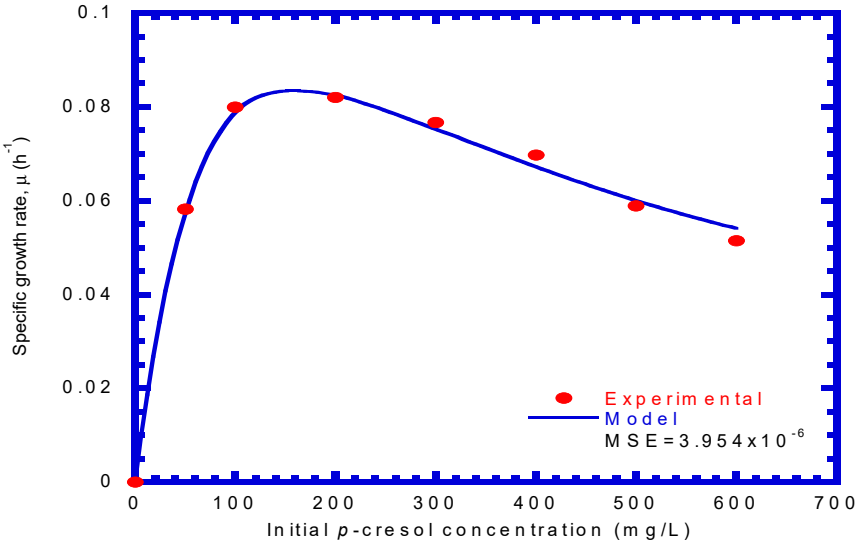


**Figure 7.** The specific growth rate of cells varied with various initial *p*-cresol concentrations. Haldane kinetics was fitted to the experimental data using the least-squares methodology. The maximum specific growth rate ($\mu_{max}$) is 0.185 $h^{-1}$, the *p*-cresol half-saturation constant is 65.1 mg/L, and the phenol inhibition constant is 243.56 mg/L.

As plotted in Figures 8 and 9, the growth yield (Y) of cells on phenol and *p*-cresol was estimated from batch tests data using Equation (3), respectively. The calculated values of Y on phenol and *p*-cresol are listed in Table 1. The growth yields on phenol were in the range of 0.337–0.343 mg $mg^{-1}$ under initial phenol concentrations ranging from 50 to 600 mg $L^{-1}$. The average growth yield on single phenol ($Y_P$) was 0.340 mg $mg^{-1}$ and the standard deviation value was 2.116 × $10^{-3}$. The growth yield on single *p*-cresol ($Y_C$) varied from 0.274 to 0.283 mg $mg^{-1}$ to acquire a mean value of 0.279 as well as a standard deviation value of 2.769 × $10^{-3}$. Abuhamed et al. [33] carried out batch tests with various initial phenol concentrations of 10–200 mg $L^{-1}$. Their experiment results revealed that the Y value was 0.44 mg $mg^{-1}$, which is greater than the Y value obtained in this study due to the lower initial phenol concentrations.

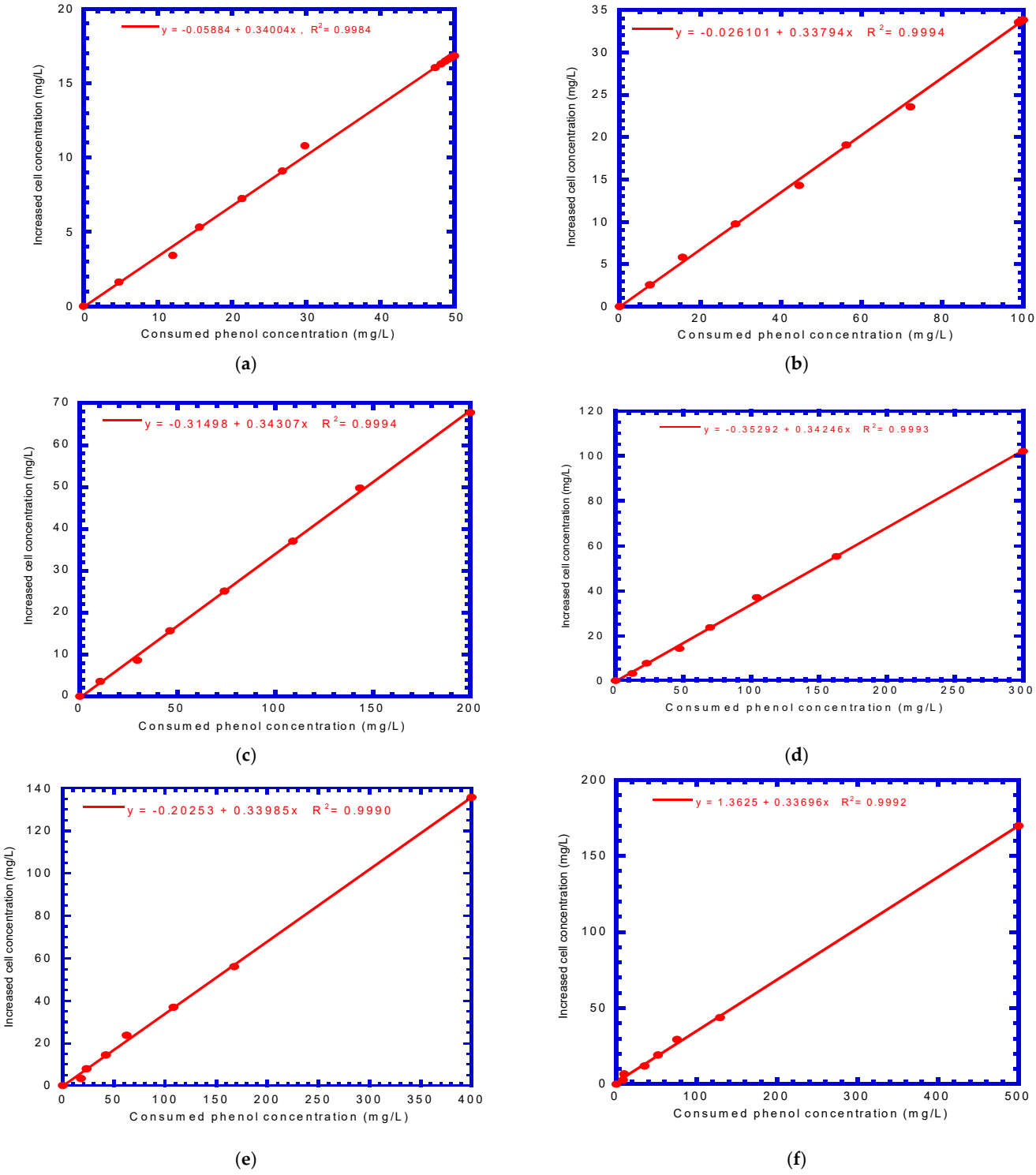


**Figure 8.** *Cont.*

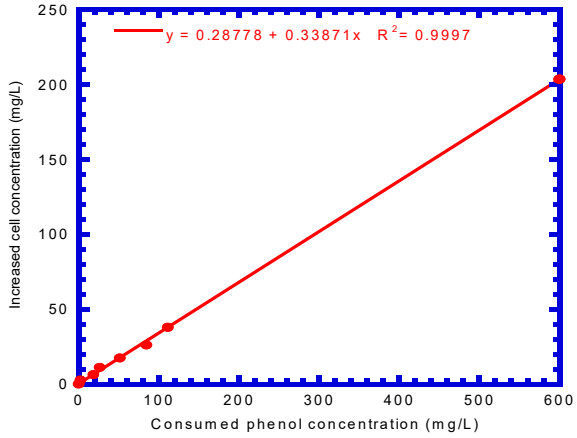


(**g**)

**Figure 8.** Batch kinetic tests to determine growth yield on phenol: (**a**) 50, (**b**) 100, (**c**) 200, (**d**) 300, (**e**) 400, (**f**) 500, and (**g**) 600 mg/L.

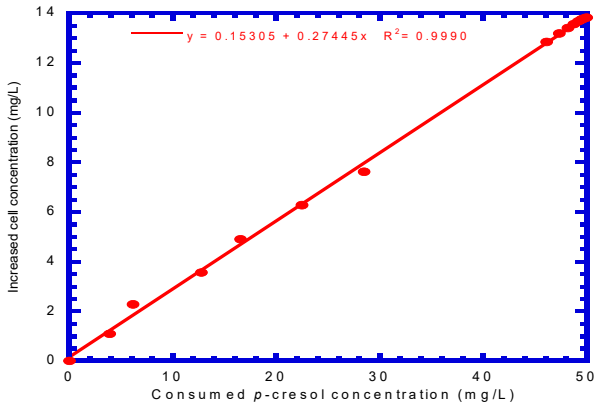


(**a**)

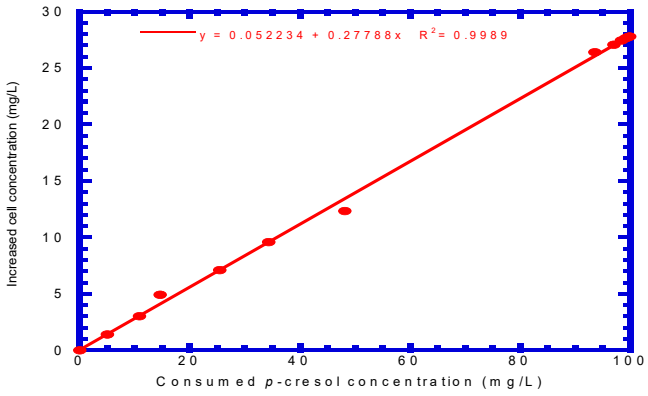


(**b**)

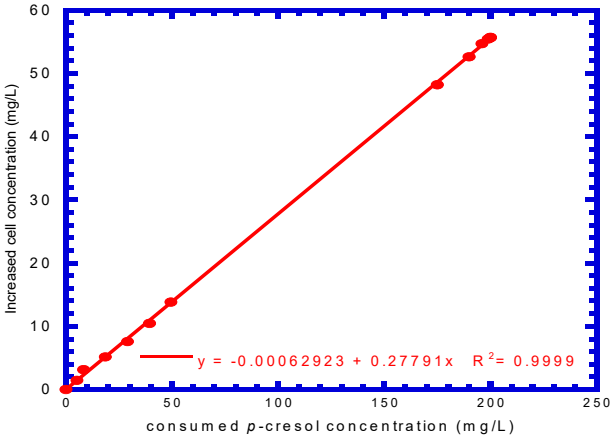


(**c**)

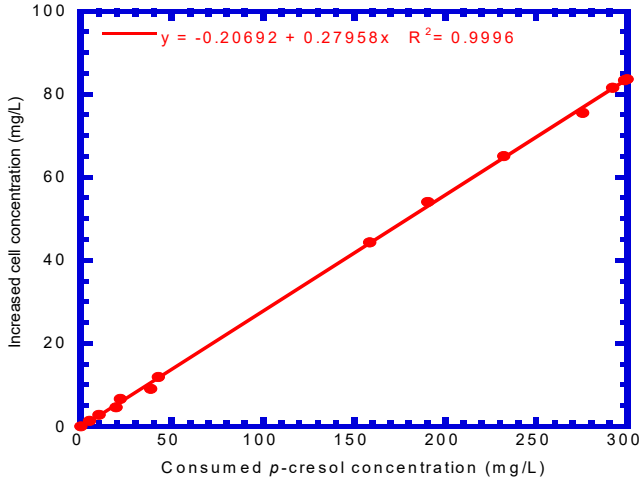


(**d**)

**Figure 9.** *Cont*.

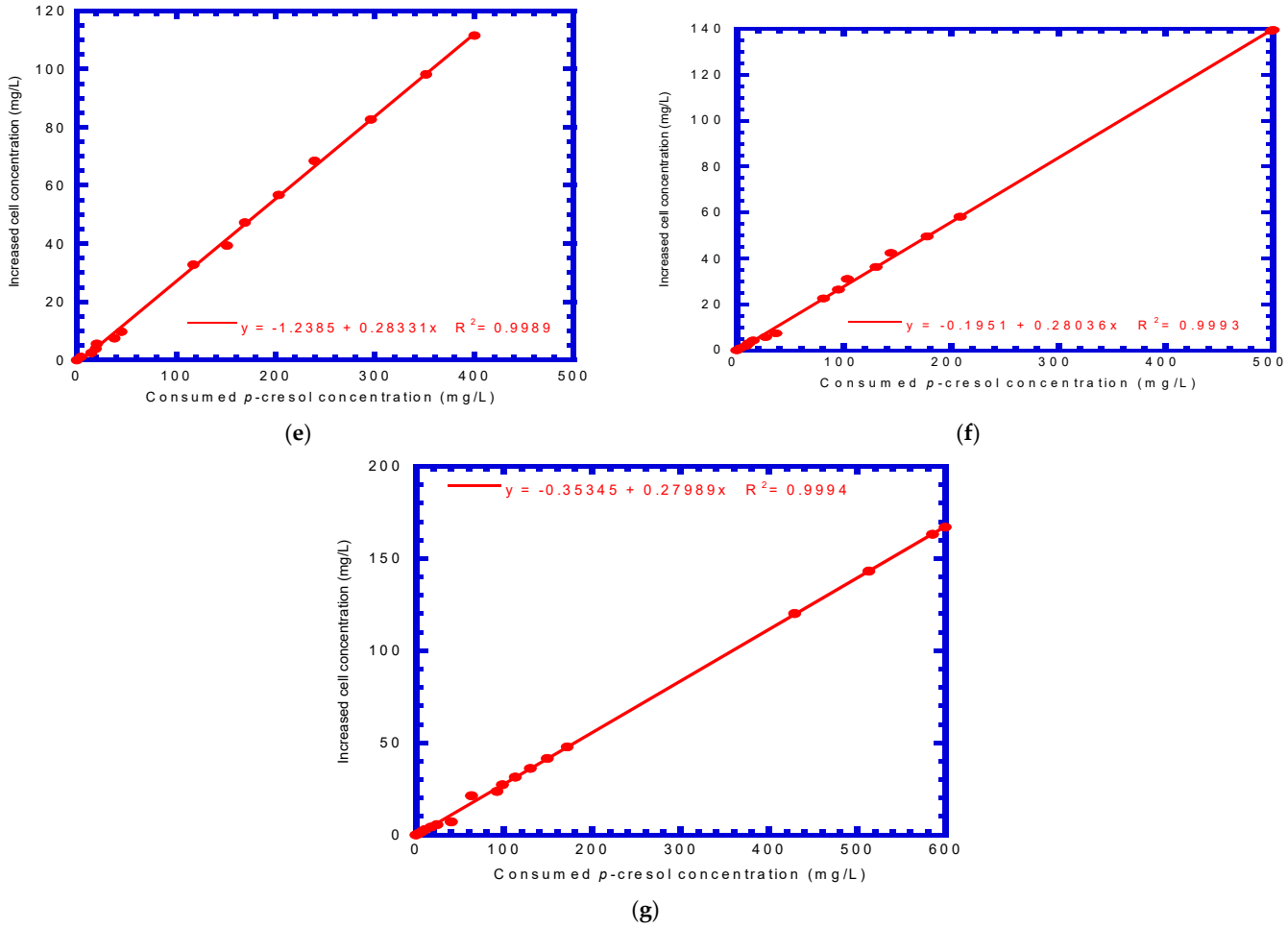


**Figure 9.** Batch kinetic tests to determine growth yield on *p*-cresol: (**a**) 50, (**b**) 100, (**c**) 200, (**d**) 300, (**e**) 400, (**f**) 500, and (**g**) 600 mg/L.

**Table 1.** Batch Tests to Evaluate Growth Yield (Y) under Various Initial Concentrations.

| Run No. | Initial Phenol Concentration (mg $L^{-1}$) | Initial *p*-Cresol Concentration (mg $L^{-1}$) | Bio-Kinetic Parameters | |
|---|---|---|---|---|
| | | | $Y_P$ (mg $mg^{-1}$) | $Y_C$ (mg $mg^{-1}$) |
| 1 | 50 | 50 | 0.340 | 0.274 |
| 2 | 100 | 100 | 0.338 | 0.278 |
| 3 | 200 | 200 | 0.343 | 0.278 |
| 4 | 300 | 300 | 0.342 | 0.280 |
| 5 | 400 | 400 | 0.340 | 0.283 |
| 6 | 500 | 500 | 0.337 | 0.280 |
| 7 | 600 | 600 | 0.339 | 0.280 |
| mean | - | - | 0.340 | 0.279 |
| standard deviation | - | - | $2.116 \times 10^{-3}$ | $2.769 \times 10^{-3}$ |

### 4.3. Phenol Plus p-Cresol in Binary Substrates System

The biodegradation of phenol plus *p*-cresol and the growth of *P. putida* cells is illustrated in Figure 10. As plotted in Figure 10a, the time required for the complete removal of phenol was 52–56 h for the initial phenol concentration ranging from 50 to 500 mg $L^{-1}$. However, the phenol removal was about 96.8% as the operating time was 56 h. As shown in Figure 10b, the time needed to remove *p*-cresol completely was 48–56 h for the initial *p*-cresol concentration between 50 and 500 mg $L^{-1}$. At the operating time of 56 h, only 79.7% removal efficiency for *p*-cresol was attained.

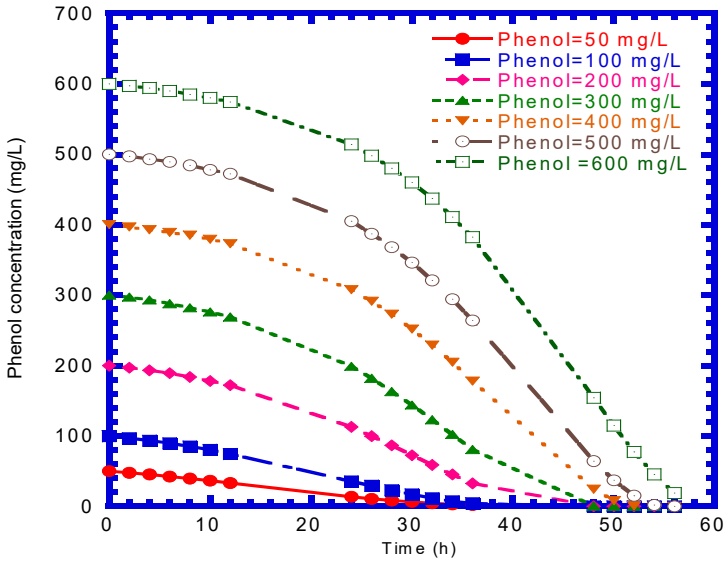


(**a**)

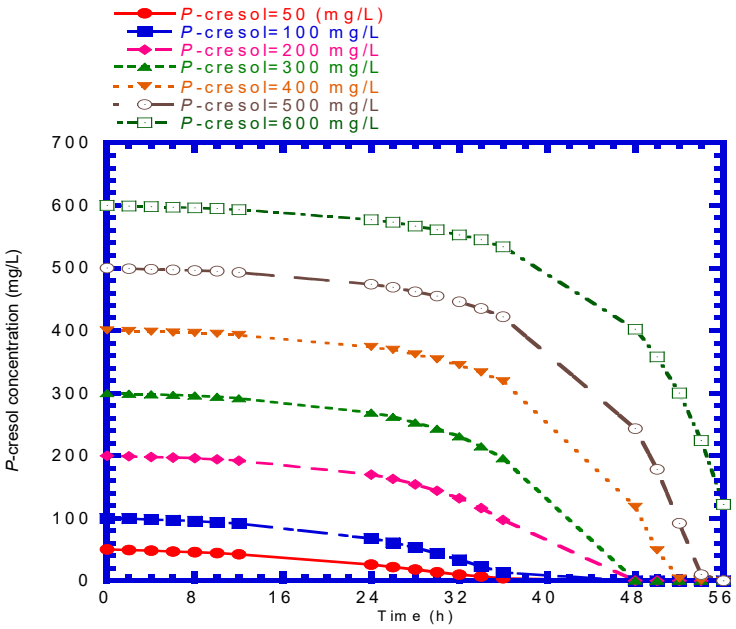


(**b**)

**Figure 10.** *Cont.*

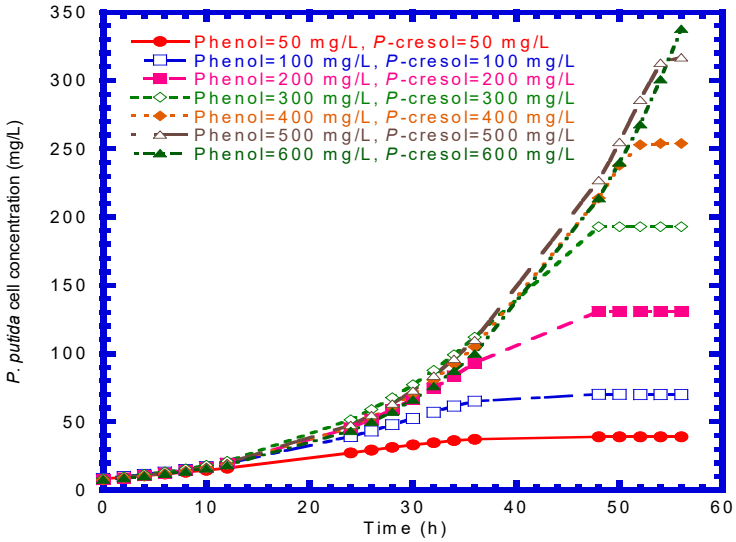


(**c**)

**Figure 10.** Batch experiments in the binary substrates system: (**a**) phenol biodegradation, (**b**) *p*-cresol biodegradation, and (**c**) *P. putida* cells growth.

Seven batch experiments were carried out at 30 °C to determine the interaction parameters of $I_{C,P}$ and $I_{P,C}$ using the non-linear least-squares regression method [27]. The cell growth in the binary system varied with time, which is plotted in Figure 10c. The specific growth rates on binary phenol plus *p*-cresol ranged from 0.185 to 0.204 $d^{-1}$ under different initial phenol and *p*-cresol contents. Figure 11 presents the specific growth rate of the cell on phenol plus *p*-cresol. The bio-kinetic parameters of $I_{C,P}$ and $I_{P,C}$ were determined by fitting experimental data to sum the model. The kinetic parameters ($\mu_m$, $K_s$, and $K_i$) in the equation are the same as those presented in the Haldane's equations for phenol and *p*-cresol biodegradation [34]. The best-fitted sum kinetic Equation (21) was given as:

$$\mu = \frac{0.45S_P}{221.4 + S_P + S_P^2/65.1 + 4.8S_C} + \frac{0.185S_C}{65.1 + S_C + S_C^2/243.56 + 12.7S_P}. \quad (21)$$

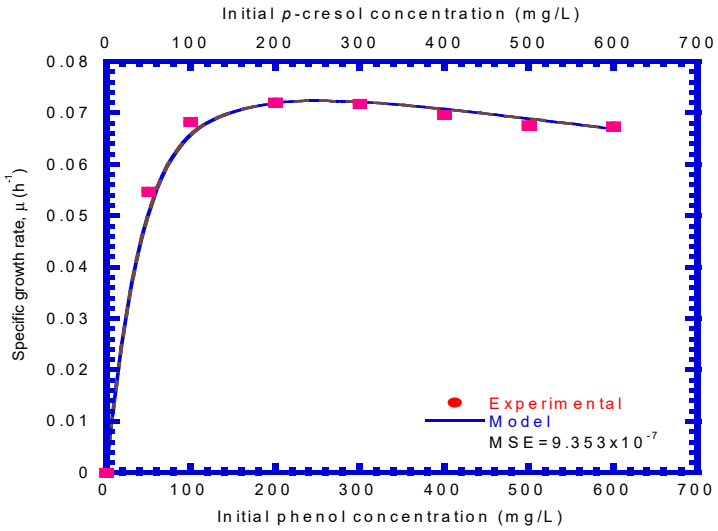


**Figure 11.** Kinetic best-fit of the specific growth rate of *P. putida* cells on the binary substrates of phenol and *p*-cresol with a correlation coefficient $R^2$ = 0.9894.

The values of $I_{C,P}$ and $I_{P,C}$ were 4.8 and 12.7, respectively, with a correlation coefficient ($R^2$) of 0.989.

### *4.4. Mass Transfer Coefficients*

Wakao and Smith [35] proposed a random pore model to determine the effective diffusivity in gel beads. Furthermore, Korgel et al. [36] used the random pore model to predict the galactose effective diffusivity in the entrapped cell system. Based on the random pore model, the effective diffusivity ($D_e$) is described as

$$D_e = D_s(1 - \beta X)^2 \tag{22}$$

where $D_s$ is the diffusion coefficient in gel beads ($cm^2\ d^{-1}$); $X$ is cell concentration ($g\ L^{-1}$); and $\beta$ is the specific volume of cells ($L\ g^{-1}$). The values of $X$ and $\alpha$ are 0.496 $g\ L^{-1}$ and $3.842 \times 10^{-3}\ L\ g^{-1}$ using the proposed measurement methods of Ju and Ho [37]. The diffusion coefficient ($D_s$) of phenol and *p*-cresol in gel beads employed in a continuous stirred-tank bioreactor is regarded as the same as that in water. The formula derived from Wilke and Chang [38] was used to calculate the values of $D_s$ for phenol and *p*-cresol, which was 0.949 and 0.856 $cm^2\ d^{-1}$, respectively. The effective diffusivity ($D_e$) of phenol and *p*-cresol was 0.945 and 0.853 $cm^2\ d^{-1}$, respectively. The following equation was applied to estimate the mass transfer coefficient $k_f$ [39]

$$k_f = \frac{Sh \cdot D_s}{d_p} \tag{23}$$

where *Sh* is Sherwood number = $\{4 + 1.21(Re)^{2/3}(Sc)^{2/3}\}^{1/2}$, *Re* is Reynolds number, and *Sc* is Schmidt number. The value of *Re* for both phenol and *p*-cresol was 38.7. The value of *Sc* for phenol and *p*-cresol was 724.7 and 803.4, respectively. The value of *Sh* for phenol and *p*-cresol was 33.48 and 34.65, respectively. By substituting these values into Equation (23), the mass transfer coefficient $k_f$ for phenol and *p*-cresol was 105.91 and 98.87 $cm\ d^{-1}$, respectively.

### *4.5. Biodegradation of Phenol and p-Cresol in Immobilized Cells*

In order to validate the kinetic model system described above, phenol and *p*-cresol concentrations in bulk liquid phase estimated by the kinetic model were compared with the experimental results under 125 $mg\ L^{-1}$ initial concentrations of phenol and *p*-cresol, respectively, in the feed. Table 2 summarized the bio-kinetic and reactor parameters as well as operating conditions applied in kinetic model simulation as reported earlier in the various batch tests.

Figure 12 plots the model-predicted and experimental data of phenol and *p*-cresol effluent concentrations against time. The effluent curve of phenol concentration consists of three segments. During a half day, the phenol and *p*-cresol concentrations increased sharply to 81.6 (0.653 $S_{b0,p}$) and 89.1 (0.713 $S_{b0,c}$) $mg\ L^{-1}$. No significant biodegradation of phenol and *p*-cresol was carried out during the half day. The phenol and *p*-cresol concentration curves were considered as the typical dilute-in curves, which is characteristic of a continuous stirred-tank bioreactor, while the bioreactor was filled with only nutrient media at the onset of the tests. The second segment of the phenol and *p*-cresol curves ran from day 0.5 to day 7, when the curves started to deviate from the peak of the dilute-in curves. The effluent concentrations of phenol and *p*-cresol leveled off and then decreased. Obviously, the immobilized cell markedly degraded phenol and *p*-cresol during this period, owing to the active growth of cells. The third segment of the phenol and *p*-cresol concentration curves ran from day 7 day 29. During this period, the immobilized cells system achieved a steady state, and the effluent concentration phenol and *p*-cresol was approximately 2.95 (0.0236 $S_{b0,p}$) and 13.63 (0.109 $S_{b0,c}$) $mg\ L^{-1}$, respectively. The removal efficiency for phenol and *p*-cresol was 97.6% and 89.1%, respectively, under a steady-state condition. The model simulations are in satisfactory agreement with the test results with a correlation coefficient ($R^2$) of 0.9392 for phenol and 0.9063 for *p*-cresol.

**Table 2.** Summary of the Biokinetic and Reactor Parameters, as well as the Operation Conditions for the Model Simulation.

| Symbol | Parameters Description (Unit) | Value | Remarks |
|---|---|---|---|
| $\varepsilon$ | reactor porosity (dimensionless) | 0.72 | measured |
| $A$ | total surface area of gel beads ($cm^2$) | $3.522 \times 10^4$ | calculated |
| $D_{eP}$ | effective diffusivity of phenol in the gel bead ($cm^2\ d^{-1}$) | 0.945 | calculated |
| $D_{eC}$ | effective diffusivity of *p*-cresol in the gel bead ($cm^2\ d^{-1}$) | 0.853 | calculated |
| $k_{fP}$ | mass-transfer coefficient of phenol ($cm\ d^{-1}$) | 105.91 | calculated |
| $k_{fC}$ | mass-transfer coefficient of *p*-cresol ($cm\ d^{-1}$) | 98.87 | calculated |
| $K_{i,P}$ | inhibition constant of phenol ($mg\ L^{-1}$) | 310.5 | measured |
| $K_{i,C}$ | inhibition constant of *p*-cresol ($mg\ L^{-1}$) | 243.56 | measured |
| $K_{s,P}$ | saturation constant of phenol ($mg\ L^{-1}$) | 221.4 | measured |
| $K_{s,C}$ | saturation constant of *p*-cresol ($mg\ L^{-1}$) | 65.1 | measured |
| $I_{C,P}$ | inhibition of cell growth on phenol due to the presence of *p*-cresol (dimensionless) | 4.8 | measured |
| $I_{P,C}$ | inhibition of cell growth on *p*-cresol due to the presence of phenol (dimensionless) | 12.7 | measured |
| $Q$ | influent flow rate ($mL\ d^{-1}$) | $6.272 \times 10^3$ | measured |
| $S_{b0,P}$ | concentration of phenol in feed ($mg\ L^{-1}$) | 125.0 | measured |
| $S_{b0,C}$ | concentration of *p*-cresol in feed ($mg\ L^{-1}$) | 125.0 | measured |
| $V$ | effective working volume (mL) | $1.568 \times 10^3$ | measured |
| $Y_P$ | growth yield of cell on phenol (mg cell [mg phenol]$^{-1}$) | 0.340 | measured |
| $Y_C$ | growth yield of cell on *p*-cresol (mg cell [mg *p*-cresol]$^{-1}$) | 0.279 | measured |
| $\mu_{max,P}$ | maximum specific growth rate of cell on phenol ($h^{-1}$) | 0.45 | measured |
| $\mu_{max,C}$ | maximum specific growth rate of cell on *p*-cresol ($h^{-1}$) | 0.185 | measured |

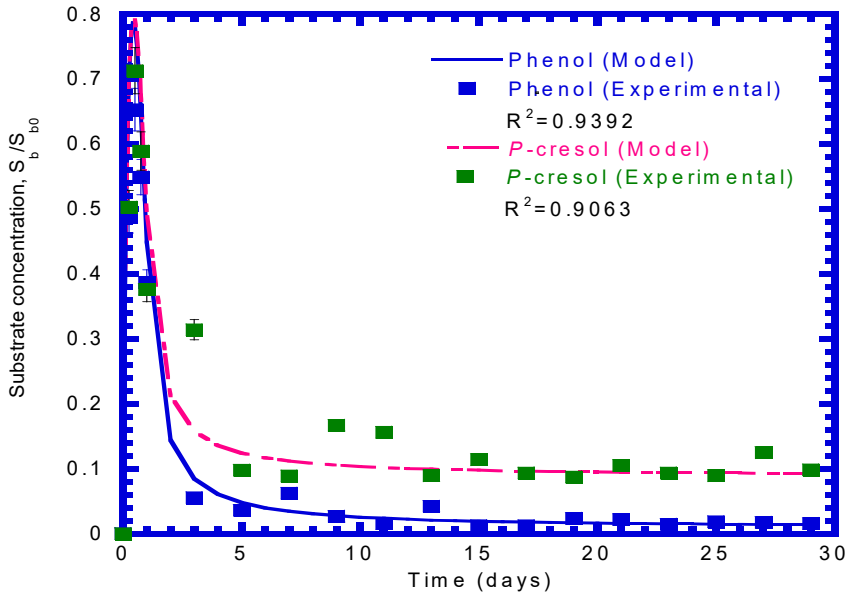


**Figure 12.** Experimental results and model prediction in phenol and *p*-cresol effluent concentrations.

The batch bioreactors were performed by Yadzir et al. [40], who found that the encapsulated cells of *Acinetobacter baumannii* in the Ca-alginate beads had the ability to remove phenol up to 2000 $mg\ L^{-1}$ within 12 d. In their study, they also found that there was no loss of Ca-alginate activity during five cycles of batch tests. Basak et al. [41] employed sugarcane bagasse as a low-cost immobilization matrix for cells entrapment in the upflow packed bed reactor to assess phenol degradation under different influent flow rates. The experimental results exhibited that the phenol removal efficiency reached up to 97%, while the feed initial phenol concentration was 2400 $mg\ L^{-1}$ and the flow rate was controlled at 4 $mL\ min^{-1}$ within the operating times of 54 h. Furthermore, Dong et al. [42] combined a zeolite imidazole framework (ZIF-8) with hydrochloric acid-modified SEP (CESEP) to form a nanocomposite CESEP/ZIF-8 for *P. putida* immobilization, which provided adsorption and biodegradation mechanisms for phenol removal. The experimental results exhibited

that phenol at initial concentrations of 10 and 20 mg $L^{-1}$ was effectively removed within 13 and 24 h as compared to 21 and 36 h for phenol removal by free *P. putida* alone.

### *4.6. Immobilized Cells Growth*

Figure 13a presents the immobilized cells growth as a function of time by model prediction. As can be seen, there is no the elapsed time required for immobilized cells to start to grow. The model predicted that the immobilized cells vigorously grew to utilized phenol at a transient-state period from 5 to 25 days. The growth of immobilized cells reached up to a maximum value of around 32 mg $L^{-1}$.

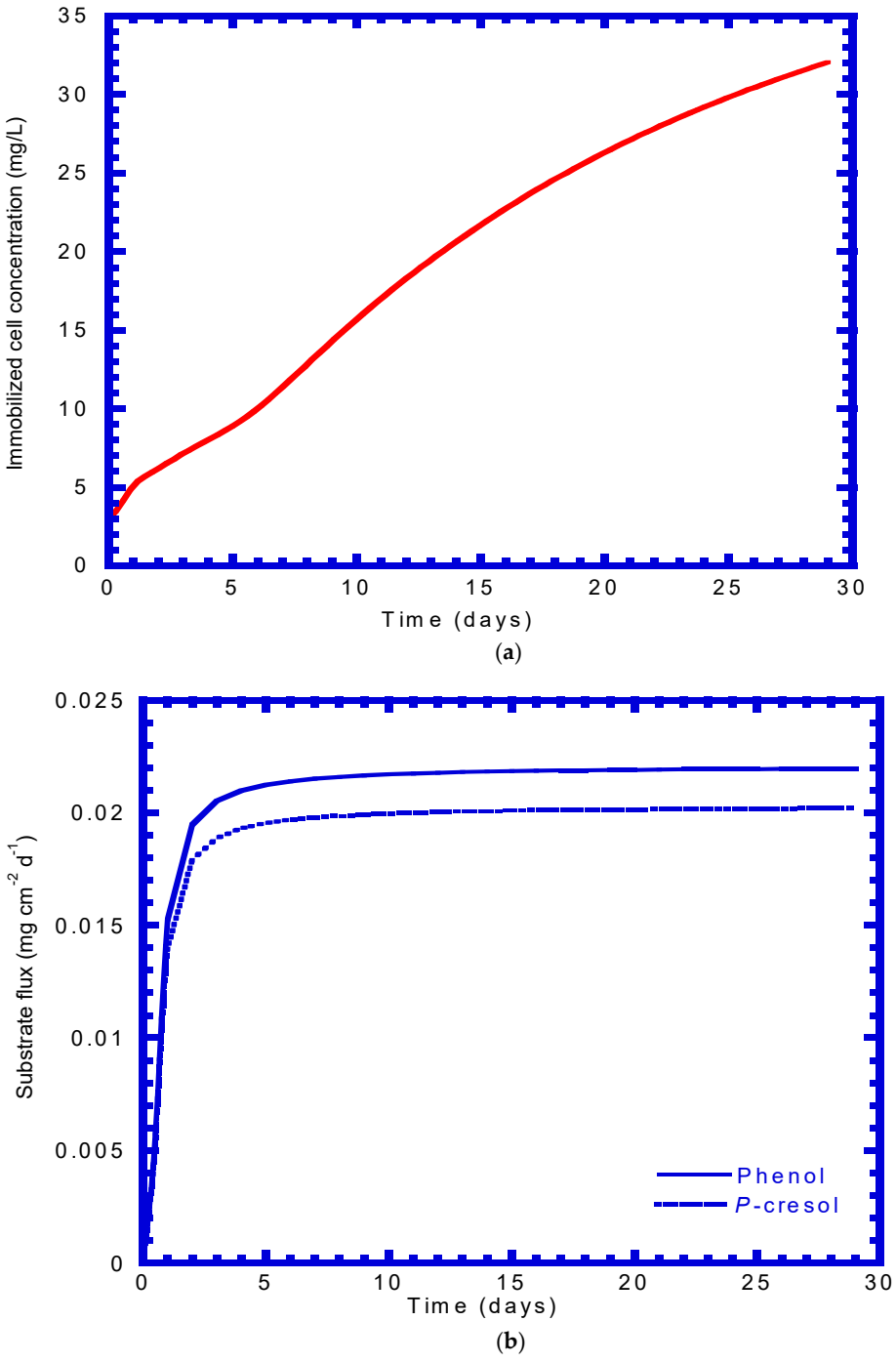


**Figure 13.** Model prediction versus time (**a**) immobilized cells growth (**b**) phenol and *p*-cresol fluxes into bead.

### *4.7. Flux into Gel Bead*

Figure 13b plots the model-predicted fluxes of phenol and *p*-cresol that diffuses from the bulk liquid into the bead. Flux represents the phenol utilization by immobilized cells. At the beginning of the experiment, the flux started at zero, and the immobilized cell growth was negligible. The flux of the immobilized cells increased abruptly at a logarithmic rate for the first four days. During this period, the immobilized cells vigorously degraded phenol and *p*-cresol in the bead—thus the difference between the concentrations of phenol and *p*-cresol in the bulk liquid and that at the bead/liquid interface increased, significantly increasing the fluxes of phenol and *p*-cresol into the beads due to biological activity. During days 4–29, the phenol and *p*-cresol concentrations in the effluent reached a constant concentration in a steady-state condition. The fluxes of phenol and *p*-cresol reached a maximal constant value, respectively, which was approximately 0.0220 and 0.0202 mg $cm^{-2}$ $d^{-1}$.

### *4.8. Phenol Concentration Profiles*

The concentration variations of phenol and *p*-cresol along the liquid film and bead phrase attained at 10, 20, and 29 days are illustrated in Figure 14. The concentration profiles for phenol and *p*-cresol due to the diffusional resistance in the liquid film and bead phases was determined by model prediction. It can be seen that phenol and *p*-cresol concentrations decreased in the liquid film and bead phases when the operating time increased. The continuous stirred-tank bioreactor achieved the steady state on day 10. The entrapped cells concentration in the bead was about 16 mg $L^{-1}$, and the cells actively utilized phenol and *p*-cresol simultaneously for their growth. The concentrations of phenol and *p*-cresol reduced promptly at 20 days around the center of bead. The values of phenol and *p*-cresol concentration approached to around zero on day 29. At this operating time, the fluxes of phenol and *p*-cresol remained a constant value, while a maximal value of the growth of entrapped cells was achieved.

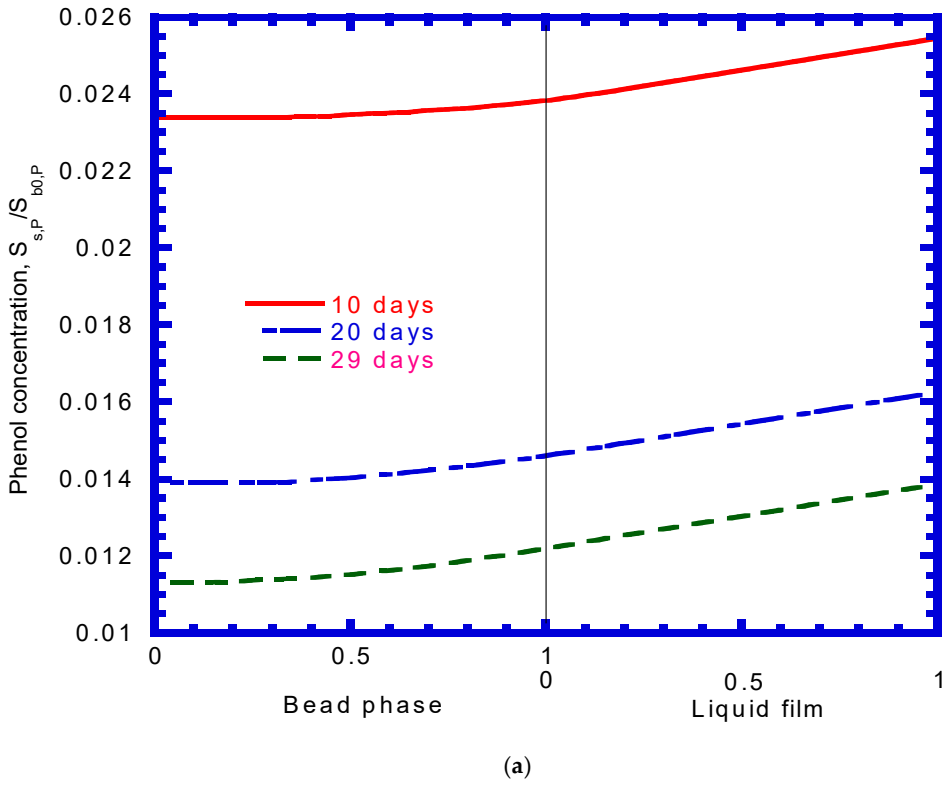


(**a**)

**Figure 14.** *Cont.*

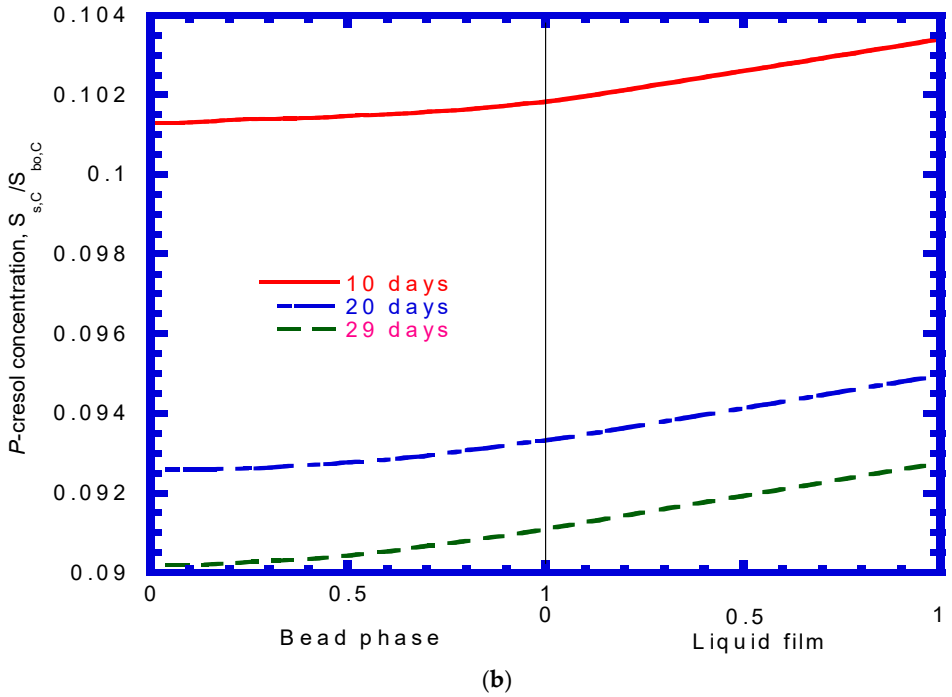


(**b**)

**Figure 14.** Model predicted phenol concentration profiles at different operating times: (**a**) phenol, (**b**) *p*-cresol.

## 5. Conclusions

The biodegradation kinetic model for the simultaneous removal of phenol and *p*-cresol was validated by conducting a continuous stirred-tank bioreactor with immobilized cells in Ca-alginate beads. Diffusion and biodegradation are two major mechanisms considered in the model system. The model agreed with experimental data very well in the continuous-flow reactor. Experimental results demonstrate that the immobilized cells process yields the high biodegradation of phenol and *p*-cresol, which was 97.6% and 89.1%, respectively. The fluxes of phenol and *p*-cresol that diffuse from the bulk liquid into the gel beads increased rapidly, while the entrapped cells in beads grew firmly during the unsteady-state period. The approaches of experiments and kinetic model presented in this study can be applied to layout a pilot-scale or full-scale entrapped cells bioreactor for the simultaneous biodegradation of phenol and *p*-cresol contaminants from various industrial wastewaters.

**Author Contributions:** Y.-H.L. conceived and designed the experiments as well as developed the kinetic models and analyzed the experimental data; Y.-J.G. conducted the batch and continuous stirred-tank bioreactors and collected the data. All authors have read and agreed to the published version of the manuscript.

**Funding:** This study was supported by a funding from the Ministry of Science and Technology of Taiwan under Contract No. MOST 108-2221-E-166-002.

**Institutional Review Board Statement:** Not applicable.

**Informed Consent Statement:** Not applicable.

**Data Availability Statement:** Not applicable.

**Conflicts of Interest:** The authors declare no conflict of interest.

## References

1. Banerjee, A.; Ghoshal, A.K. Phenol degradation performance by isolated *Bacillus cereus* immobilized in alginate. *Int. Biodeterior. Biodegrad.* **2011**, *65*, 1052–1060. [CrossRef]
2. Sahoo, N.K.; Pakshirajan, K.; Ghosh, P.K. Enhancing the biodegradation of 4-chlorophenol by *Arthrobacter chlorophenolics* A6 via medium development. *Int. Biodeterior. Biodegrad.* **2010**, *64*, 474–480. [CrossRef]

3. Mollaei, M.; Abdollahpour, S.; Atashgahi, S.; Abbasi, H.; Masoomi, F.; Rad, I.; Lotfi, A.S.; Zahiri, H.S.; Vali, H.; Noghabi, K.A. Enhanced phenol degradation by *pseudomonas* sp. SA01: Gaining insight into the novel single and hybrid immobilizations. *J. Hazard. Mater.* **2010**, *175*, 284–292. [CrossRef] [PubMed]
4. Kulkarni, M.; Chaudhari, A. Biodegradation of p-nitro phenol by *P. putida*. *Bioresour. Technol.* **2006**, *97*, 982–988. [CrossRef] [PubMed]
5. Pakshirajan, K.; Chugh, D.; Saravanan, P. Feasibility of m-cresol degradation using an indigenous mixed microbial culture with glucose as co-substrate. *Clean Technol. Environ. Policy* **2007**, *10*, 303–308. [CrossRef]
6. Bai, J.; Wen, J.P.; Li, H.M.; Jiang, Y. Kinetic modeling of growth and biodegradation of phenol and *m*-cresol using *Alcaligenes faecalis*. *Process Biochem.* **2007**, *42*, 510–517. [CrossRef]
7. Masque, C.; Nolla, M.; Bordons, A. Selection and adaptation of a phenol degrading strain of *Pseudomonas*. *Biotechnol. Lett.* **1987**, *9*, 655–660. [CrossRef]
8. Soda, S.; Ike, M.; Fujita, M. Effects of inoculation of a sequencing batch activated sludge process treating phenol. *J. Ferment. Bioeng.* **1998**, *86*, 90–96. [CrossRef]
9. Aksu, Z.; Bülbül, G. Determination of the effective diffusion coefficient of phenol in Ca-alginate-immobilized *P. putida* beads. *Enzym. Microb. Technol.* **1999**, *25*, 344–348. [CrossRef]
10. Loh, K.C.; Chung, T.S.; Wei-Fern, A. Immobilized-cell membrane bioreactor for high-strength phenol wastewater. *J. Environ. Eng.* **2000**, *126*, 75–79. [CrossRef]
11. Jiangliang, X.; Yanan, W.; Shi, K.; Xiao, X.; Gao, Y.; Li, L.; Qiao, Y. Study on the degradation performance and kinetics of immobilized cells in straw-alginate beads in marine environment. *Bioresour. Technol.* **2019**, *280*, 88–94.
12. Parvanova-Mancheva, T.; Vasileva, E.; Beschkov, V.; Gerginova, M.; Stoilova-Disheva, M.; Alexieva, Z. Biodegradation potential of *Pseudomonas putida* to phenol compared to *Xanthobacter autotrophicus* GJ10 and *Pseudomonas denitrificans* strains. *J. Chem. Technol. Metall.* **2020**, *55*, 23–27.
13. González, G.; Herrera, G.; García, M.T.; Peña, M. Biodegradation of phenolic industrial wastewater in a fluidized bed bioreactor with immobilized cells of *Pseudomonas putida*. *Bioresour. Technol.* **2001**, *80*, 137–142. [CrossRef]
14. Yu, Y.G.; Loh, K.C. Inhibition of *p*-cresol on aerobic biodegradation of carbazole and sodium salicylate by *Pseudomonas putida*. *Water Res.* **2002**, *36*, 1794–1802. [CrossRef]
15. Loh, K.C.; Ranganath, S. External-loop fluidized bed airlift bioreactor (EFBAB) for the cometabolic biotransformation of 4-chlorophenol (4-cp) in the presence of phenol. *Chem. Eng. Sci.* **2005**, *60*, 6313–6319. [CrossRef]
16. Singh, U.; Arora, N.K.; Sachan, P. Simultaneous biodegradation of phenol and cyanide present in coke-oven effluent using immobilized *Pseudomonas putida* and *Pseudomonas stutzeri*. *Brazil. J. Microbiol.* **2018**, *49*, 38–44. [CrossRef]
17. Ehrhardt, H.M.; Rehm, H.J. Semicontinuous and continuous degradation of phenol by *Pseudomonas putida* P8 adsorbed on activated carbon. *Appl. Environ. Microbiol.* **1989**, *30*, 312–317. [CrossRef]
18. Chen, K.C.; Lin, Y.H.; Chen, W.H.; Liu, Y.C. Degradation of phenol by PAA-immobilized *Candida tropicalis*. *Enzym. Microb. Technol.* **2002**, *31*, 490–497. [CrossRef]
19. Chung, T.P.; Wu, C.Y.; Juang, R.S. Improved dynamic analysis on cell growth with substrate inhibition using two-phase models. *Biochem. Eng. J.* **2005**, *25*, 209–217. [CrossRef]
20. Bera, S.; Kauser, H.; Mohanty, K. Optimization of *p*-cresol biodegradation using novel bacterial strains from petroleum hydrocarbon fallout. *J. Water Process Eng.* **2019**, *31*, 1–6. [CrossRef]
21. Arya, D.; Kumar, S.; Kumar, S. Biodegradation dynamics and cell maintenance for the treatment of resorcinol and *p*-cresol by filamentous fungus *Gliomastix indicus*. *J. Hazard. Mater.* **2011**, *198*, 49–56. [CrossRef] [PubMed]
22. Yoon, H.; Klinzing, G.; Blanch, H.W. Competition for mixed substrates by microbial populations. *Biotechnol. Bioeng.* **1977**, *19*, 1193–1210. [CrossRef] [PubMed]
23. Xiao, M.T.; Huang, Y.Y.; Ye, J.; Guo, Y.H. Study on the kinetic characteristics of the asymmetric production of R-(−)-mandelic acid with immobilized *Saccharomyces cerevisiae* FD11b. *Biochem. Eng. J.* **2008**, *39*, 311–318. [CrossRef]
24. González, G.; Herrera, M.G.; García, M.T.; Peña, M.M. Biodegradation of phenol in a continuous process: Comparative study of stirred tank and fluidized-bed bioreactors. *Bioresour. Technol.* **2001**, *76*, 245–251. [CrossRef]
25. Wang, S.W.; Loh, K.C.; Chua, S.S. Prediction of critical cell growth behavior of *Pseudomonas putida* to maximize the cometabolism of 4-chlorophenol with phenol and sodium glutamate as carbon source. *Enzym. Microb. Technol.* **2003**, *32*, 422–430. [CrossRef]
26. Panigrahy, N.; Barik, M.; Sahoo, R.K.; Sahoo, N.K. Metabolic profile analysis and kinetics of *p*-cresol biodegradation by an indigenous Pseudomonas citronellolis NS1 isolated from coke oven wastewater. *Int. Biodeterior. Biodegrad.* **2020**, *147*, 1–9. [CrossRef]
27. Juang, R.S.; Tsai, S.Y. Growth kinetics of *Pseudomonas putida* in the biodegradation of single and mixed phenol and sodium salicylate. *Biochem. Eng. J.* **2006**, *31*, 133–140. [CrossRef]
28. Kumar, A.; Kumar, S.; Kumar, S. Biodegradation kinetics of phenol and catechol using *Pseudomonas putida* MTCC 1194. *Biochem. Eng. J.* **2005**, *22*, 151–159. [CrossRef]
29. Wang, S.J.; Loh, K.C. Modeling the role of metabolic intermediates in kinetics of phenol biodegradation. *Enzym. Microb. Technol.* **1999**, *25*, 177–184. [CrossRef]
30. Chung, T.P.; Tseng, H.Y.; Juang, R.S. Mass transfer effect and intermediate detection for phenol degradation in immobilized *Pseudomonas putida* systems. *Process Biochem.* **2003**, *38*, 1497–1507. [CrossRef]

31. Monteiro, A.A.; Boaventura, R.A.; Rodrigues, A.E. Phenol biodegradation by *Pseudomonas putida* DSM 548 in a batch reactor. *Biochem. Eng. J.* **2000**, *6*, 45–49. [CrossRef]
32. Banerjee, I.; Modak, J.M.; Bandopadhyay, K.; Das, D.; Maiti, B.R. Mathematical model for evaluation of mass transfer limitations in phenol biodegradation by immobilized *Pseudomonas putida*. *J. Biotechnol.* **2001**, *87*, 211–223. [CrossRef]
33. Abuhamed, T.; Bayraktar, E.; Mehmetoğlu, T.; Mehmetoğlu, Ü. Kinetics model for growth of *Pseudomonas putida* F1 during benzene, toluene and phenol biodegradation. *Process Biochem.* **2004**, *39*, 983–988. [CrossRef]
34. Saravanan, P.; Pakshirajan, K.; Saha, P. Biodegradation of phenol and m-cresol in a batch and fed batch operated internal loop airlift bioreactor by indigenous mixed microbial culture predominantly *Pseudomonas* sp. *Bioresour. Technol.* **2008**, *99*, 8553–8558. [CrossRef] [PubMed]
35. Wakao, N.; Smith, J.M. Diffusion and reaction in porous catalysts. *Ind. Eng. Chem. Fund.* **1964**, *2*, 123–127. [CrossRef]
36. Korgel, B.A.; Rotem, A.; Monbonquett, H.G. Effective diffusivity of galactose in calcium alginate gels containing immobilized *Zymonmonas mobilis*. *Biotechnol. Prog.* **1992**, *8*, 111–117. [CrossRef] [PubMed]
37. Ju, L.K.; Ho, C.S. Correlation of cell volume fractions with cell concentrations in fermentation media. *Biotechnol. Bioeng.* **1988**, *32*, 95–99. [CrossRef]
38. Wilke, C.E.; Chang, P. Correlation of diffusion coefficients in dilute solutions. *AIChE J.* **1955**, *1*, 264–270. [CrossRef]
39. Brian, P.L.T.; Hales, H.B. Effect of transpiration and changing diameter on heat and mass transfer to sphere. *AIChE J.* **1969**, *15*, 419–425. [CrossRef]
40. Yadzir, Z.H.M.; Shukor, M.Y.; Ahmad, A.; Nazir, M.S.; Shah, S.M.U.; Abdullah, M.A. Phenol removal by newly isolated *Acinetobacter baumannii* strain Serdang 1 in a packed-bed column reactor. *Desalination Water Treat.* **2016**, *57*, 13307–13317. [CrossRef]
41. Basak, B.; Jeon, B.H.; Kurade, M.B.; Saratale, G.D.; Bhunia, B.; Chatterjee, P.K.; Dey, A. Biodegradation of high concentration phenol using sugarcane bagasse immobilized *Candida tropicalis* PHB5 in a packed-bed column reactor. *Ecotoxicol. Environ. Saf.* **2019**, *180*, 317–325. [CrossRef] [PubMed]
42. Dong, R.; Chen, D.; Li, N.; Xu, Q.; Li, H.; He, J.; Lu, J. Removal of phenol from aqueous solution using acid-modified *Pseudomonas putida*-sepiolite/ZIF-8 bio-nanocomposites. *Chemosphere* **2020**, *239*, 124708. [CrossRef] [PubMed]